Supplementary information

First Report on Crystal Engineering of Hg(II)halides with Fully Substituted 3,4-Pyridinedicarboxamides: Generation of 2D Coordination Polymers And Linear Zig-zag Chains of Mercury Metal Ions.

Love Karan Rana, Sanyog Sharma, Geeta Hundal*

Department of Chemistry, UGC sponsored centre of advance studies-I, Guru Nanak Dev University, Amritsar-143005, Punjab, India.

lovekaranrana@yahoo.com ; **sharma.sanyog@yahoo.com**; **geetahundal@yahoo.com**

Table of Contents

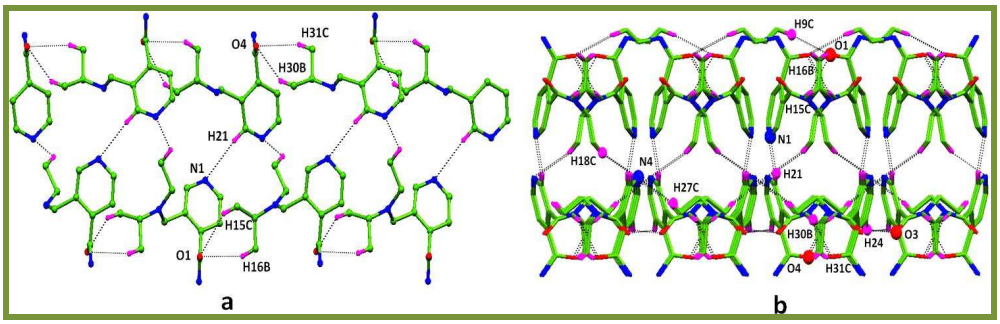

Fig. S1. (a) Parallel helical chains of **L1** due to C-H···O interactions. Only one chain from each crystallographically independent molecule is shown. Further helical tape formation is shown due to (py to py) C21-H21···N1 H-bonding interactions between these chains. (b) 2D H-bonded network formed by mutual C-H···O H-bonding among the helical tapes, shown in the *bc* plane.

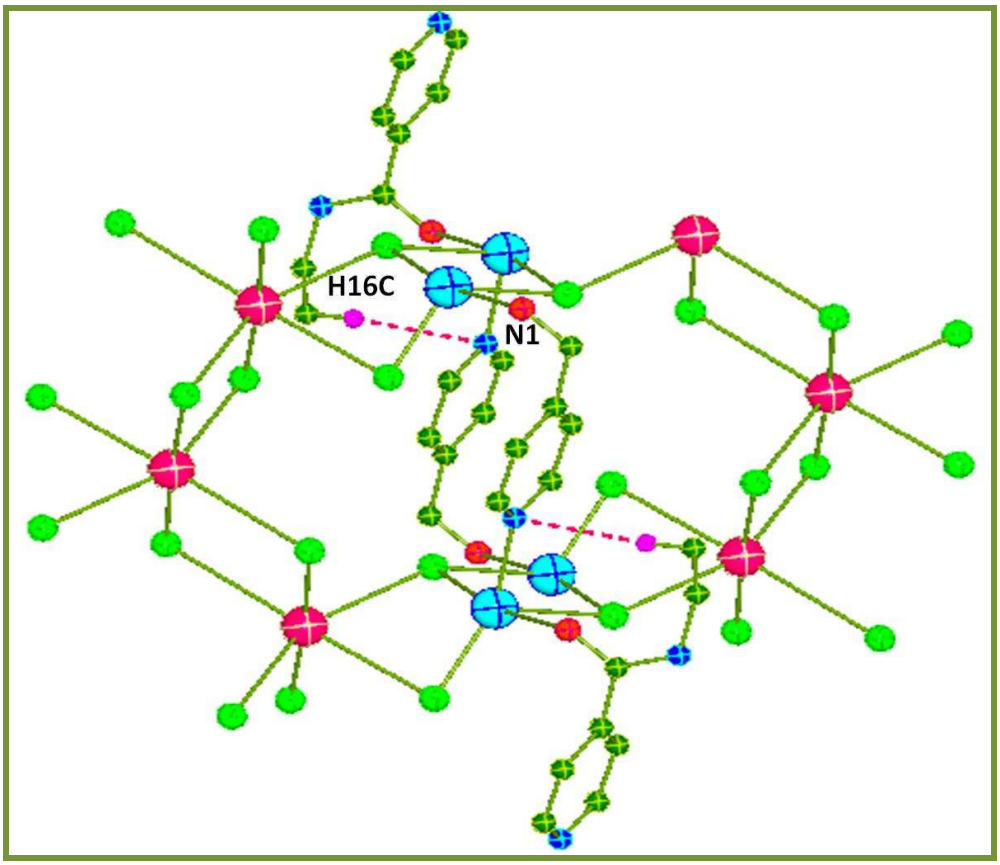

Fig. S2. Showing the C16-H16C···N(py) H-bonding interactions.

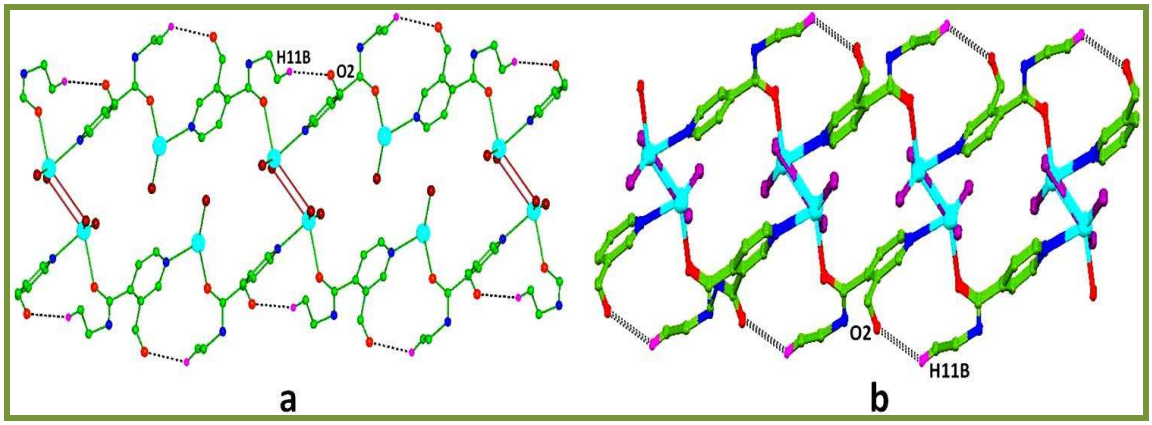

Fig. S3. Showing C-H···O interactions in (a) complex **2** (b) complex **3.**

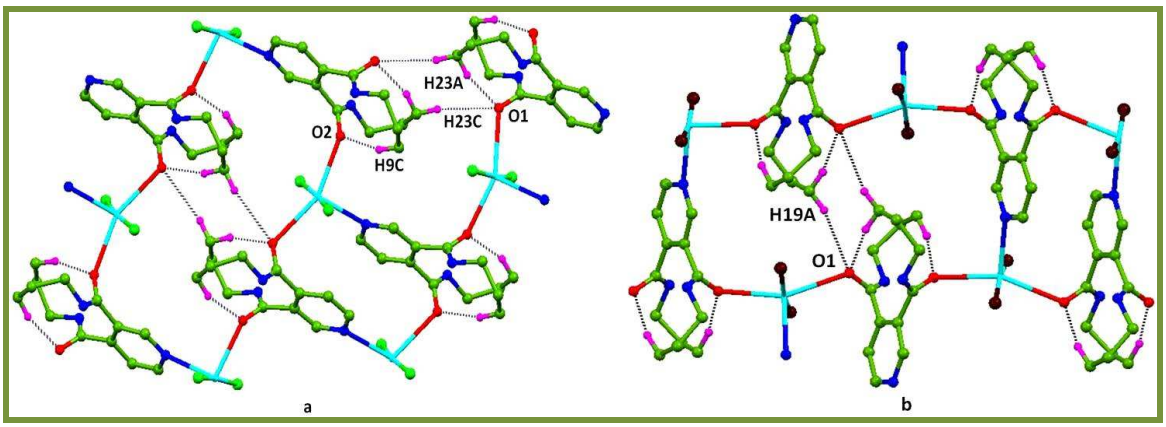

Fig. S4. Showing C-H···O interactions in (a) complex **4** (b) complex **5.**

Table S1. Showing relevant C-H···π interactions in the complexes.

Complex	D—H···A	A···H/ Å	A···D/ Å	A···H—D/°
1	C16-H16 ···Py^{i}	2.89	3.75	148
2	C12-H12B··· Py^{i}	3.19	4.06	148
4	C22-H22B··· Py^{i}	3.17	4.01	147
5	C18-H18C··· Py^{i}	3.19	4.04	146

(**1**) i: x+1,+y,+z ,(**2**): i: x,-y+1/2,+z+1/2, (**4**): i : -x+1/2,+y+1/2,-z+1/2,

(**5**): i : -x+1/2,+y-1/2,-z+1/2+1

Table S2. Parameters for estimating π···π interactions between two pyridine rings in the complexes.

Complex	Cg-Cg(Å)	α (°)	β(°)	$d_{\text{plane}\cdots\text{plane}}$ (Å)	d_{offset}
4	4.17	0.0	27.39	3.70	1.92
5	4.10	0.0	26.74	3.67	1.84

*Cg-Cg is the centroid to centroid distance of the two rings, β is the displacement or offset angle i.e the angle between the Cg-Cg vector and the ring normal, α is the dihedral angle between two planes containing pyridine rings, d_{offset} is the horizontal displacement from face to face alignment, two values if two rings are not exactly parallel (α ≠ 0).

Table S3: Showing various C-H···O/N H-bonding interactions in **L1**.

D—H···A	A···H/ Å	A···D/ Å	A···H—D/ deg
C9-H9C···O1[i]	2.96	3.879(15)	161
C15-H15C···O1[ii]	2.76	3.621(12)	150
C31-H31C···O4[ii]	2.73	3.598(11)	151
C18-H18C···N4[ii]	2.90	3.482(15)	120
C30-H30B···O4[ii]	2.71	3.586(12)	152
C16-H16B···O1[ii]	2.70	3.575(11)	151
C24-H24···O3[iii]	2.97	3.669(10)	132
C27-H27C···N4[iv]	2.97	3.901(13)	164
C8-H8A···O2	2.82	3.619(15)	142
C11-H11C···O1	2.49	3.011(13)	114
C12-H12B···O1	2.46	2.996(13)	115
C15-H15B···O2	2.39	2.976(11)	119
C16-H16C···O2	2.48	3.040(14)	117
C19-H19A···O1	2.82	3.640(13)	144
C21-H21···N1	2.68	3.600(14)	168
C27-H27A···O4	2.64	3.485(11)	147
C30-H30C···O3	2.45	3.006(11)	116
C31-H31B···O3	2.45	3.007(11)	116
C35-H35A···O3	2.79	3.642(13)	149
C37-H37C···O4	2.39	2.983(14)	120
C38-H38B···O4	2.35	2.955(13)	120

Symmetry code: i: x,+y+1,+z, ii: x-1/2,-y,+z, iii: x+1/2,-y+1,+z, iv : x,+y-1,+z

Table S4: Showing various C-H···O/N H-bonding interactions in complex **1**.

D—H···A	A···H/ Å	A···D/ Å	A···H—D/ deg
C8-H8A···O2	2.67	3.420(12)	135
C15-H15B···O2	2.45	3.017(15)	117
C16-H16C···O2	2.48	3.026(11)	116
C11-H11B···O1	2.39	2.957(16)	118
C12-H12C···O1	2.48	3.023(14)	116
C18-H18A···O1	2.61	3.395(17)	139
C16- H16C···N1[i]	2.86	3.816(15)	171

Symmetry code : i : x-1,+y,+z

Table S5: Showing various C-H···O H-bonding interactions in complex **2**.

D—H···A	A···H/ Å	A···D/ Å	A···H—D/ deg
C11-H11C···O1	2.49	3.036(7)	115
C12-H12B···O1	2.38	2.951(7)	117
C14-H14···O1	2.86	3.587(7)	130
C7-H7···O2	2.66	3.291(7)	121
C8-H8A···O2	2.60	3.193(7)	119
C18-H18B···O2	2.41	2.987(9)	117
C19-H19C···O2	2.44	3.006(8)	116
C11-H11B···O2^{i}	2.76	3.474(8)	130

Symmetry code: i : x,-y+1/2,+z-1/2

Table S6: Showing various C-H···O H-bonding interactions in complex **3**.

D—H···A	A···H/ Å	A···D/ Å	A···H—D/ deg
C11-H11C···O1	2.42	2.975(9)	117
C12-H12B···O1	2.49	3.031(10)	116
C18-H18A···O1	2.99	3.659(12)	127
C7-H7···O2	2.81	3.324(11)	114
C8-H8A···O2	2.48	3.173(13)	128
C15-H15B···O2	2.42	2.981(12)	117
C16-H16C···O2	2.45	3.012(15)	117
C11-H11B···O2^{i}	2.99	3.571(11)	120

Symmetry code : i : x,-y+1/2,+z-1/2

Table S7: Showing various C-H···O H-bonding interactions in complex **4**.

D—H···A	A···H/ Å	A···D/ Å	A···H—D/ deg
C23-H23C···O1	2.85	3.704(9)	149
C23-H23A···O1^{i}	2.73	3.675(8)	167
C9-H9C···O2	2.70	3.555(11)	148

Symmetry code: i**:** -x,-y,-z.

Table S8: Showing various C-H···O H-bonding interactions in complex **5**.

D—H···A	A···H/ Å	A···D/ Å	A···H—D/ deg
C19 -H19A···O1[i]	2.73	3.679(9)	162
C13-H13B···O2	2.58	3.468(11)	151
C16-H16A···O2	2.32	2.768(10)	106

Symmetry code: i: -x,-y+2,-z+1

Table S9: Showing various C-H···O H-bonding interactions in complex **6**.

D—H···A	A···H/ Å	A···D/ Å	A···H—D/ deg
C9-H9B···O2	2.62	3.385(14)	137
C21-H21···O1[i]	2.89	3.535(11)	124
C5 -H5···O2[ii]	2.73	3.474(9)	138

Symmetry code: i : -x+1,-y,-z+1 ii : x,+y+1,+z

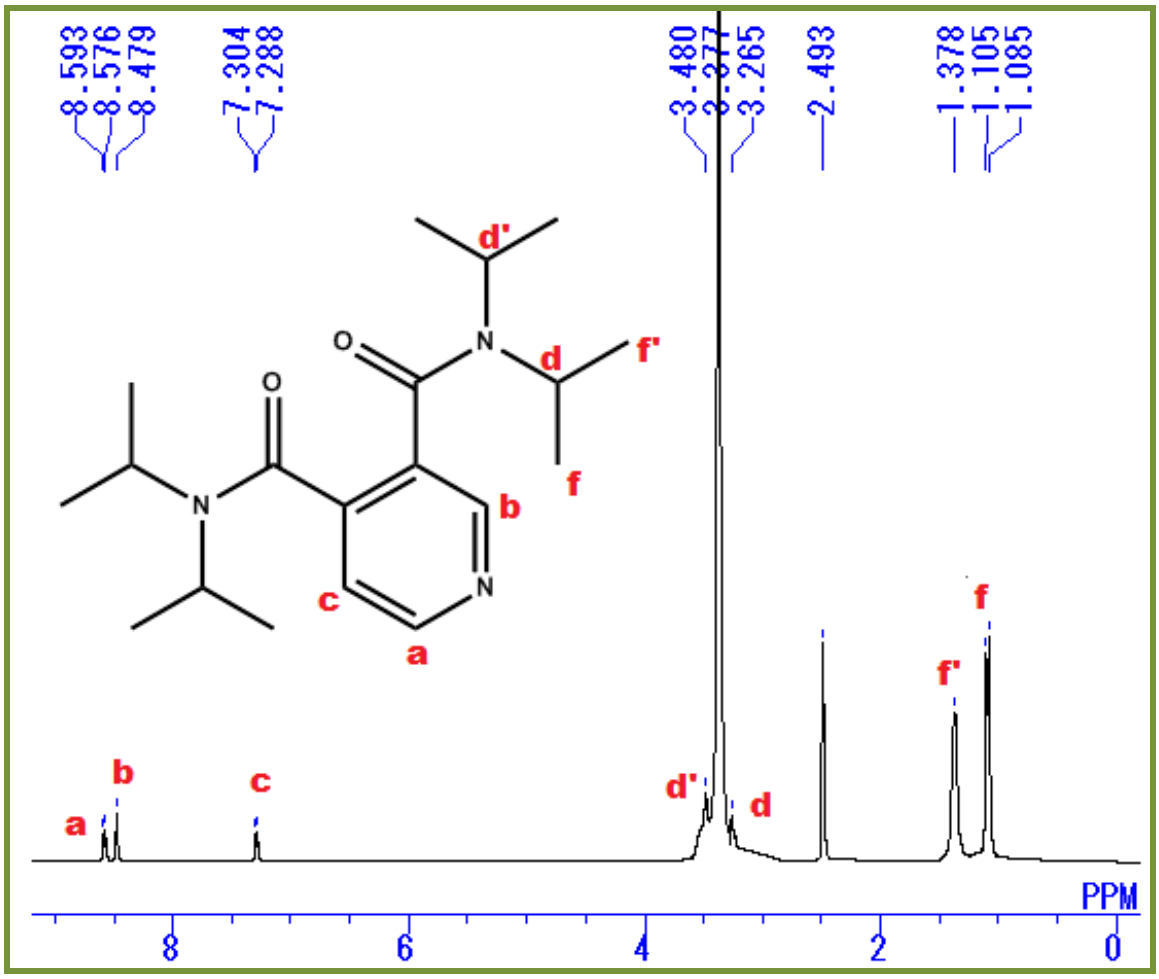

Fig. S5. ^{1}H NMR of L1 in DMSO-d$_6$.

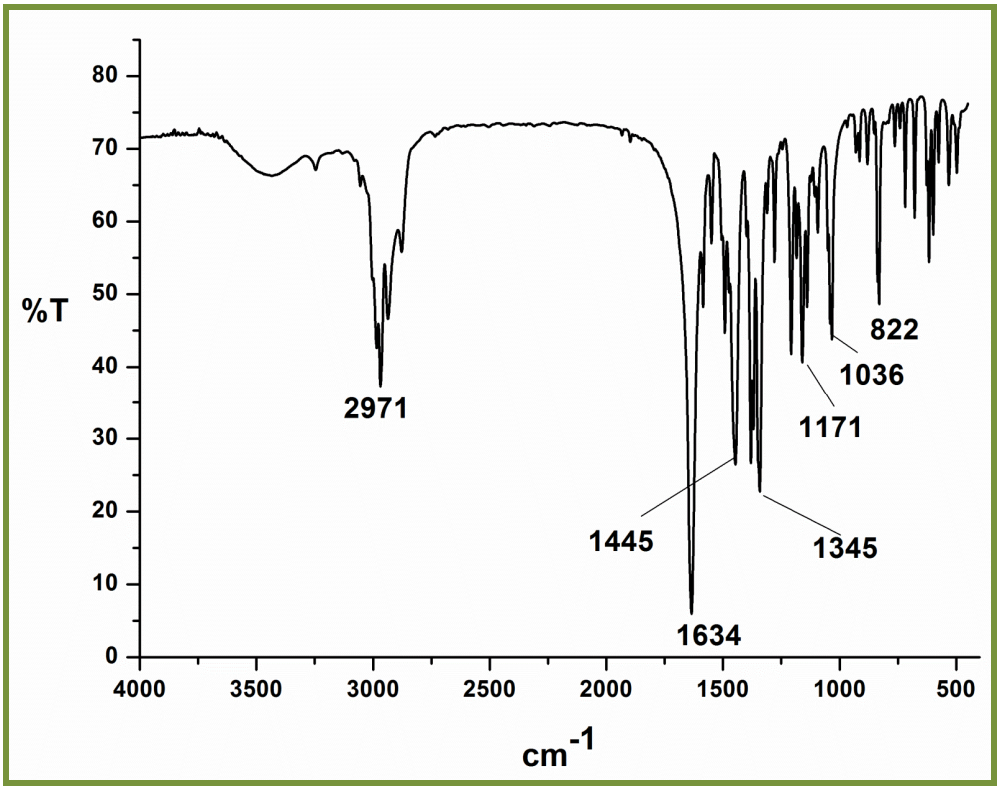

Fig. S6. IR spectrum of L1.

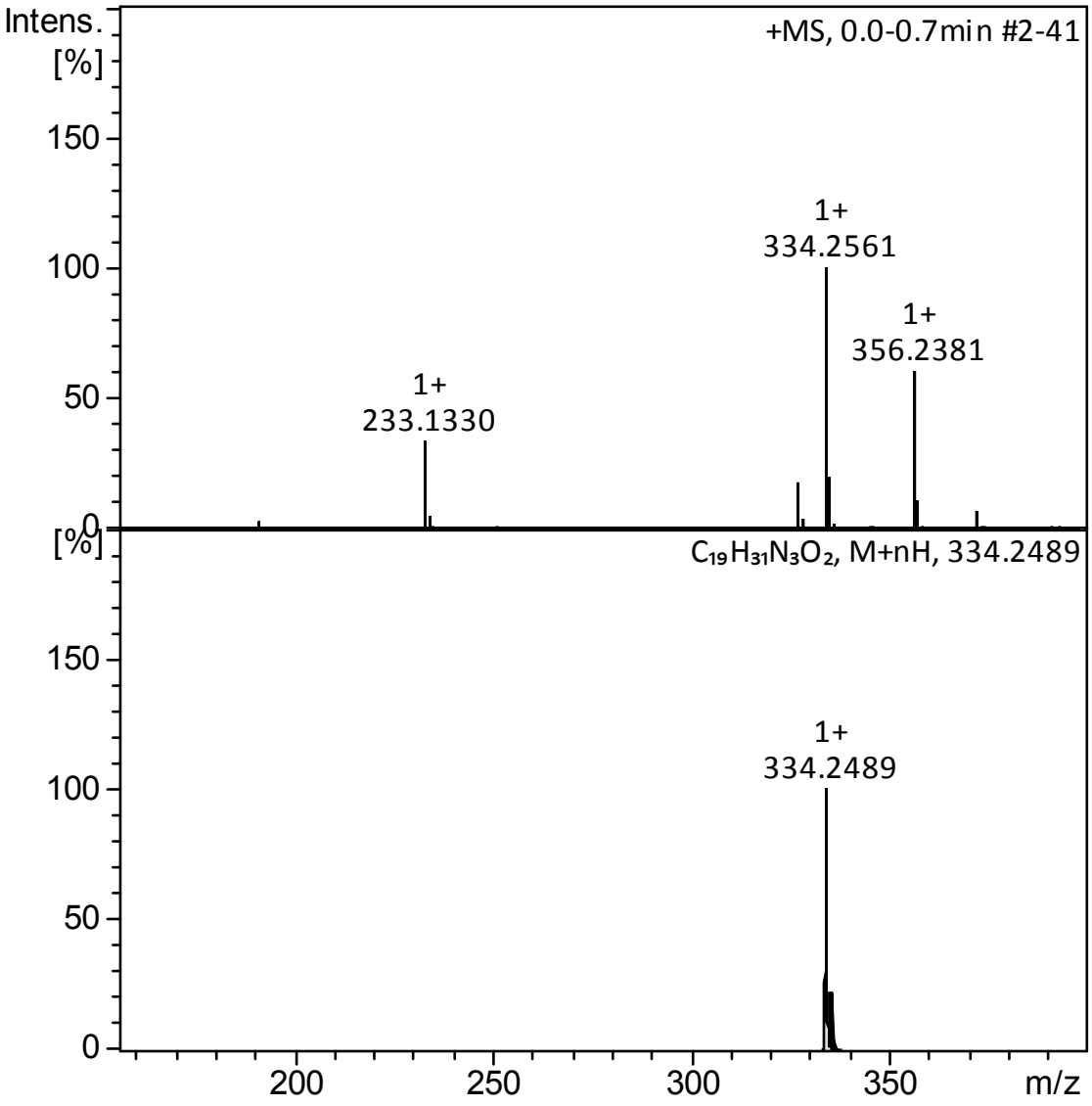

Fig. S7. Mass spectrum of L1.

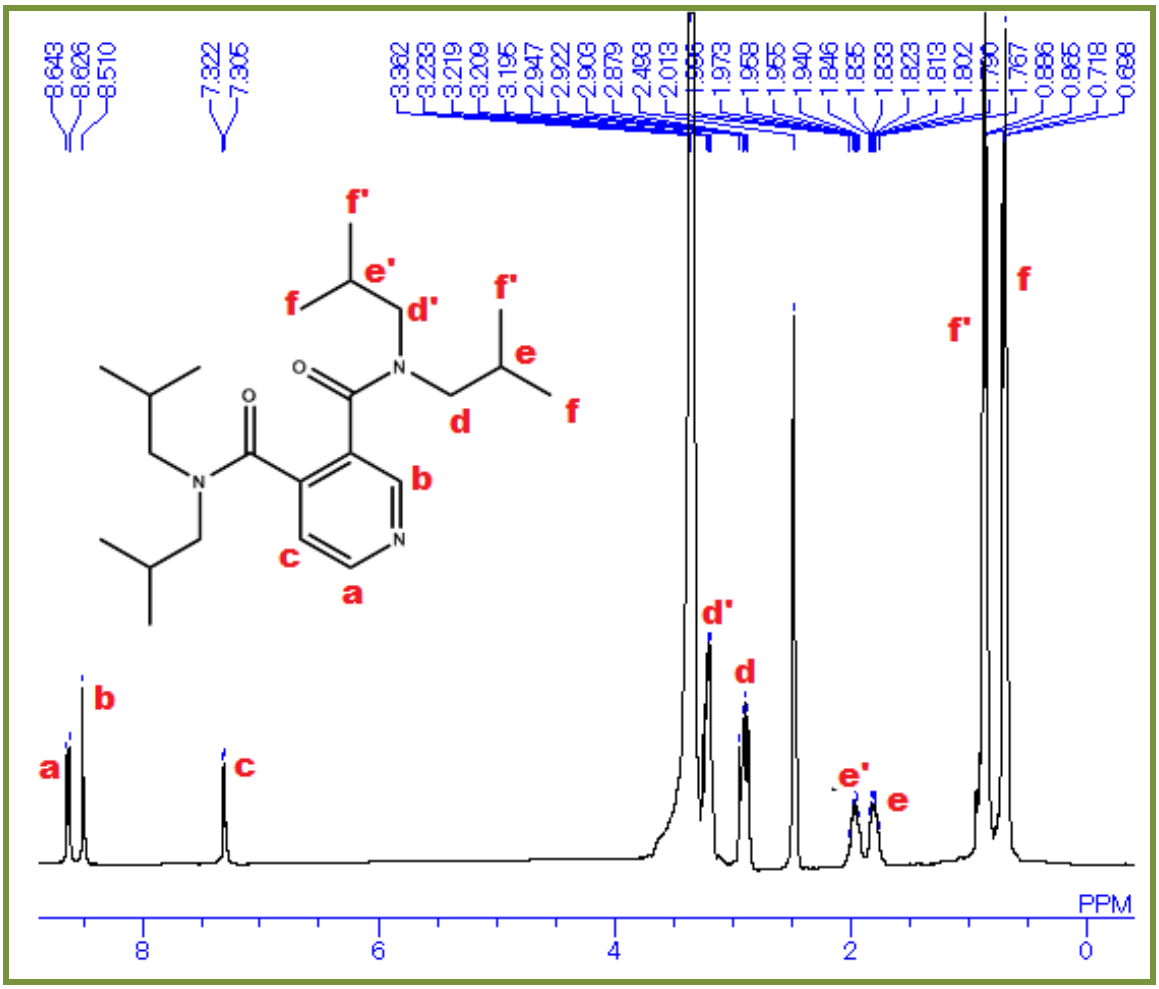

Fig. S8. ^{1}H NMR of L2 in DMSO-d$_6$.

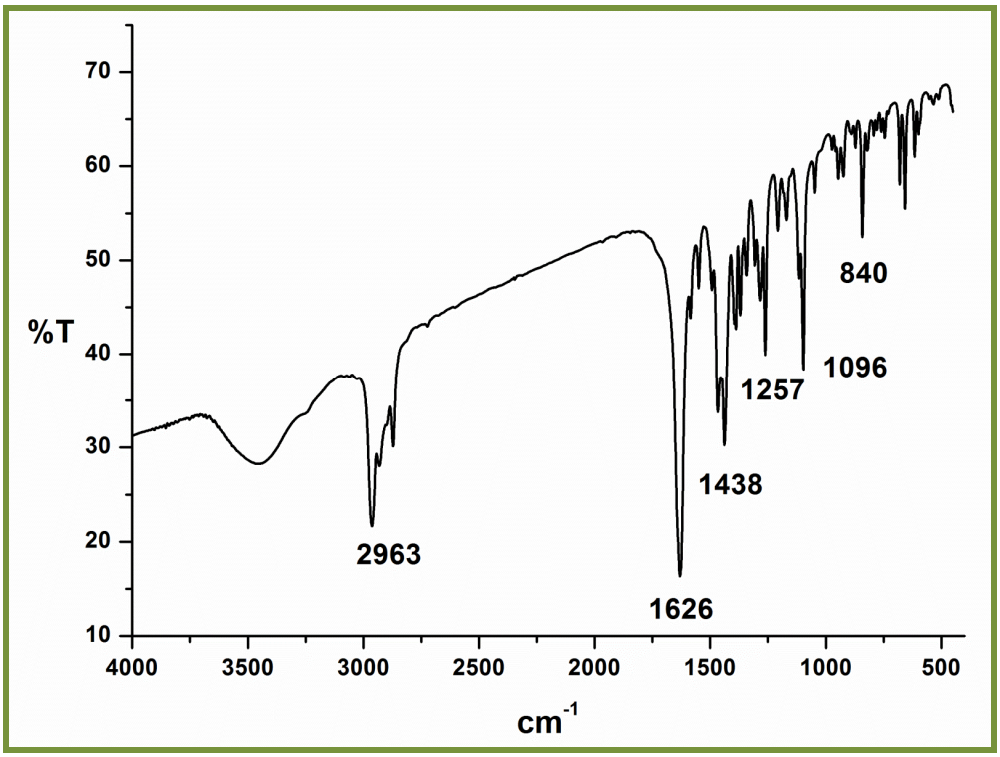

Fig. S9. IR spectrum of L2.

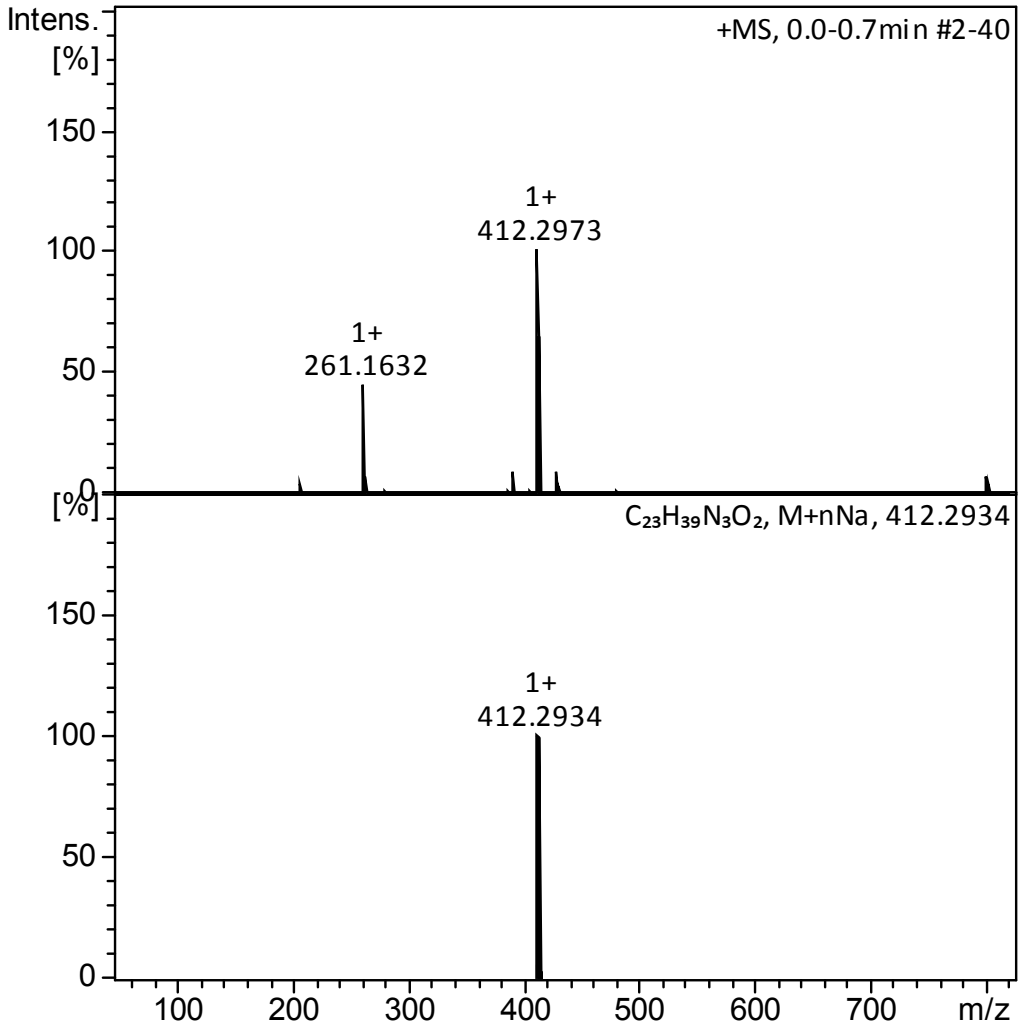

Fig. S10. Mass spectrum of L2.

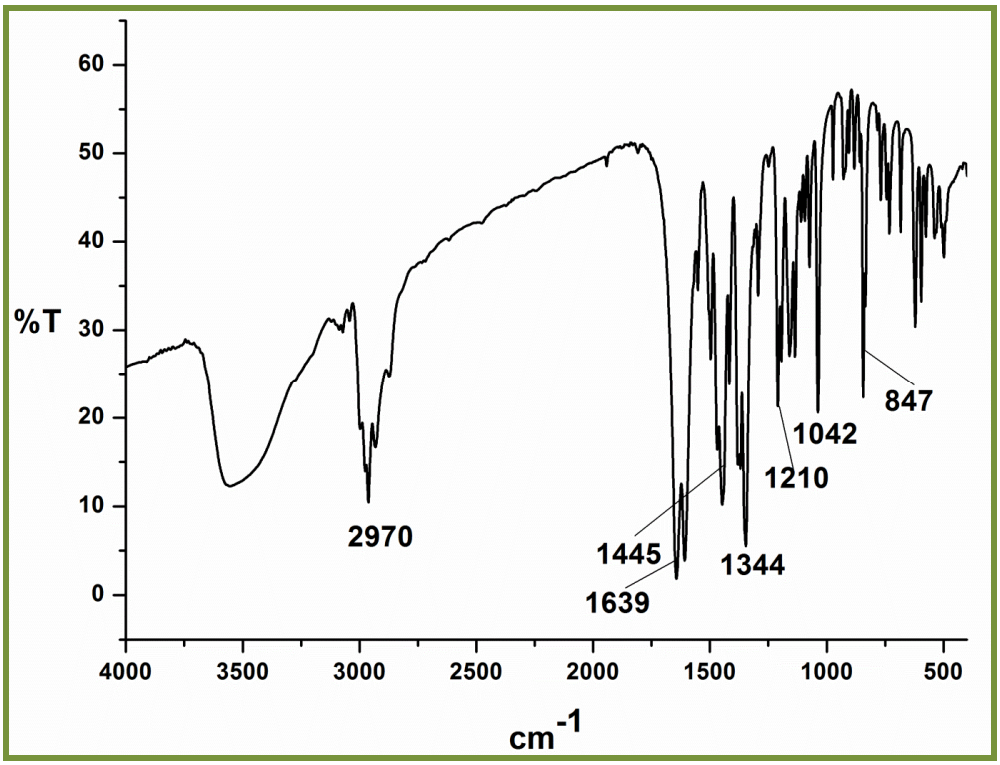

Fig. S11. IR spectrum of complex 1.

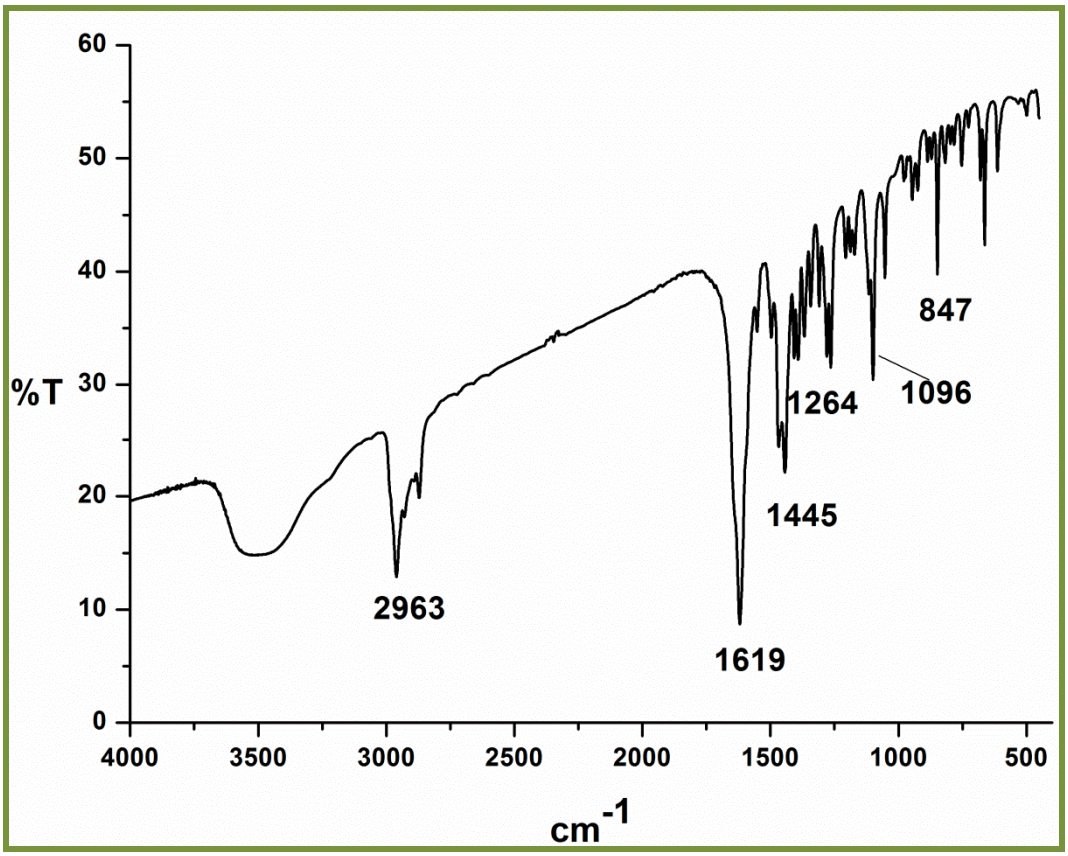

Fig. S12. IR spectrum of complex 4.

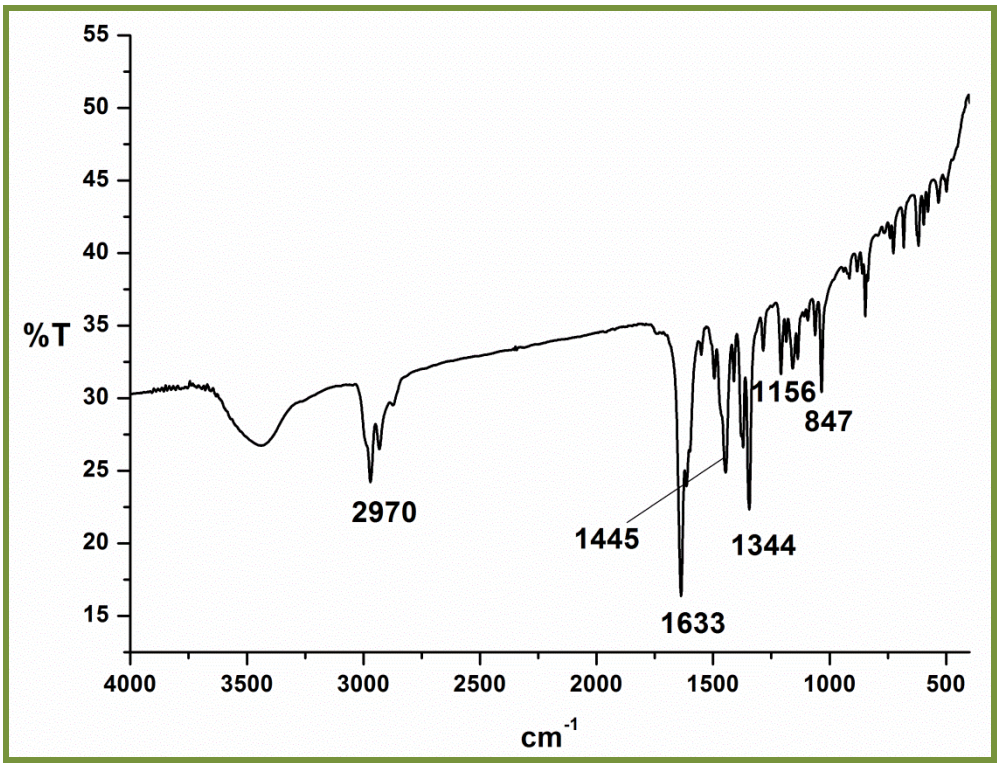

Fig. S13. IR spectrum of complex 2.

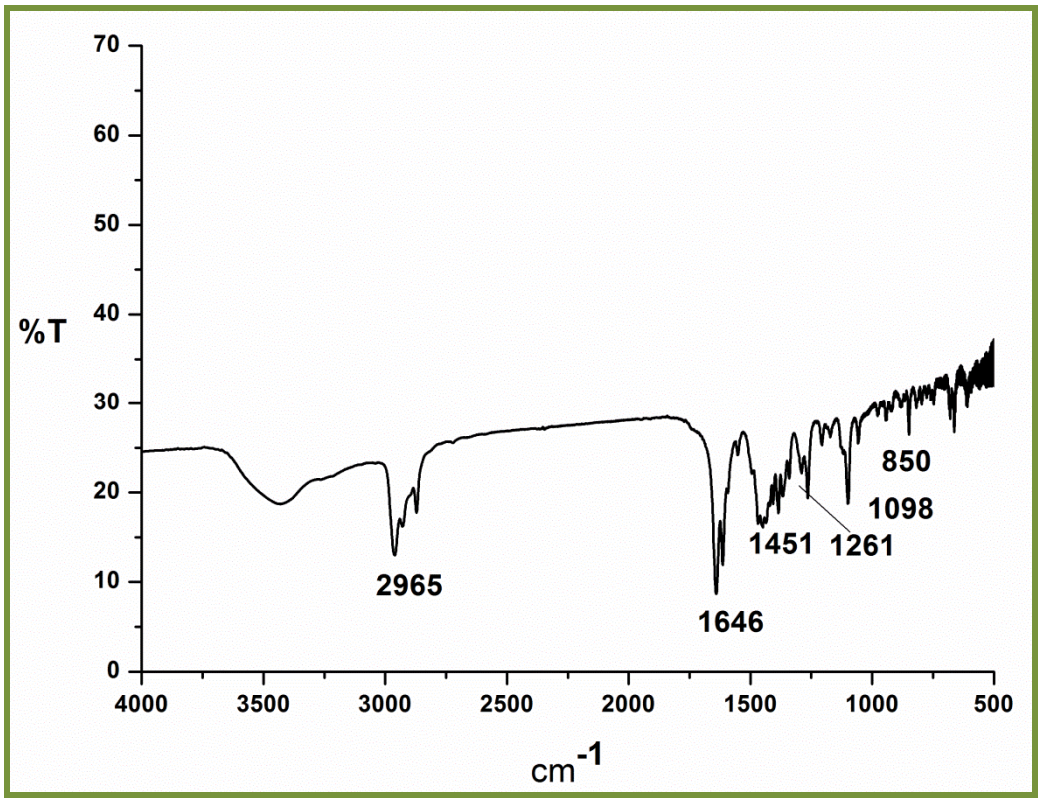

Fig. S14. IR spectrum of complex 5.

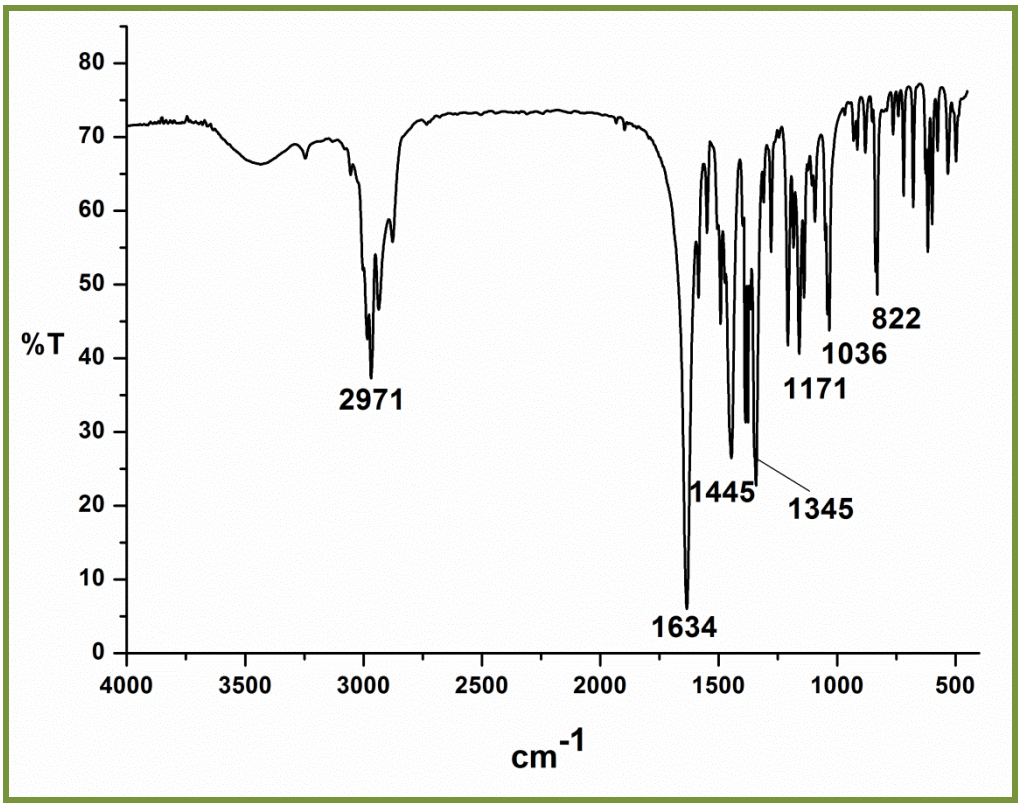

Fig. S15. IR spectrum of complex 3.

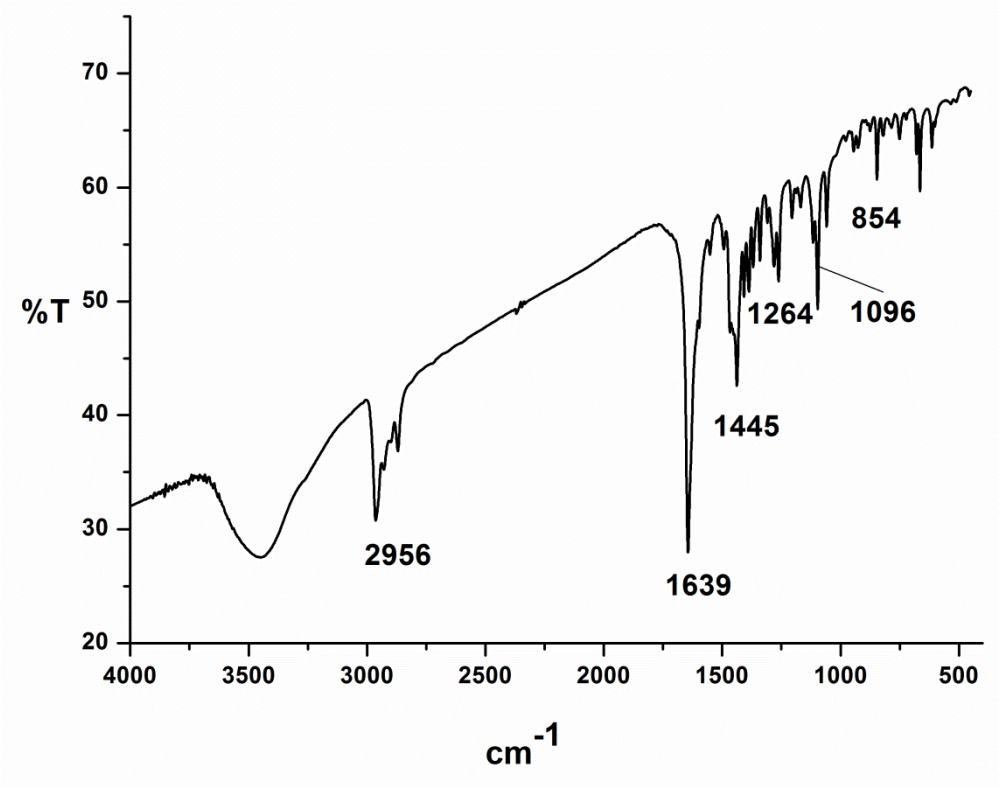

Fig. S16. IR spectrum of complex 6.

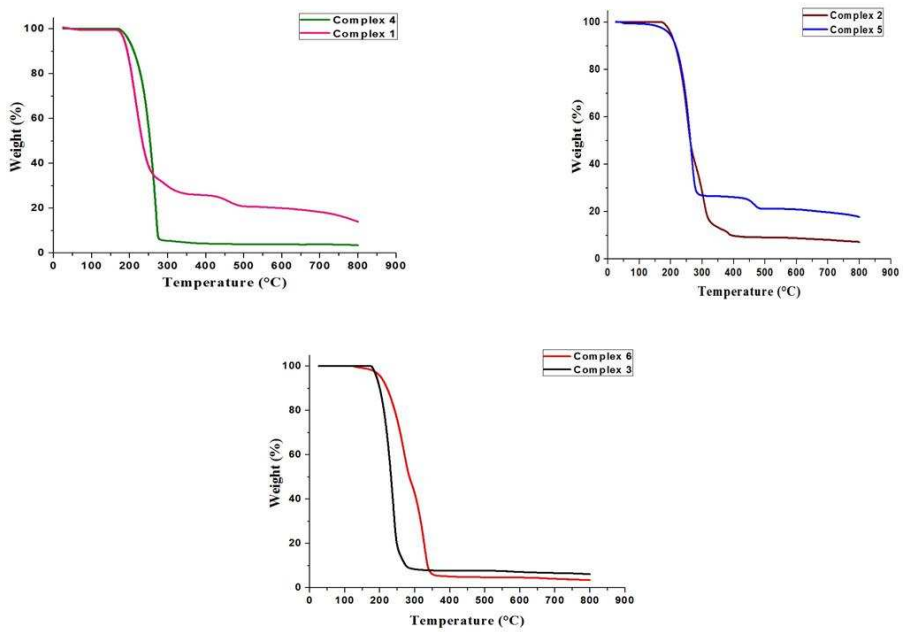

Fig. S17. TGA plots for complexes 1-6.

The thermostability of the compounds vis-à-vis their dimensionality was studied with the help of TGA experiments. TGA studies on complexes show that 1-5 are stable up to ~170 ^{o}C after which they decompose in one or two steps to yield, HgO, Hg metal or completely decompose. Complex **1**, having two different kinds of Hg(II) ions shows that it is stable up to 171 ^{o}C and beyond which it undergoes decomposition with a weight loss (obs. wt. loss, 73.9 %) up to 364 ^{o}C corresponds to Hg**L1**Cl_3 unit (calc. wt. loss, 73.0 %). From 364 ^{o}C onwards till 489 ^{o}C the weight loss corresponds to one chloride ion leaving behind mercury metal (obs. wt. loss 4.9; calc. wt. loss, 4.1 %). The TGA curve of complex **2** shows that the complex is stable up to 177 ^{o}C. Beyond this temperature it loses weight very rapidly and gets decomposed on heating up to 400 ^{o}C. Complex **3** decomposes in one step after 176 ^{o}C leaving behind metallic mercury as the residue (obs. wt. loss, 87.5; calc. wt. loss, 86.9 %). Complex **4** shows a steep fall in the curve after 173 ^{o}C rapid weight loss of the complex with almost a complete loss of weight up to 290 ^{o}C. TGA of complex **5** shows it to be stable up to 173 ^{o}C subsequently it loses weight in two consecutive steps up to 480 ^{o}C. The weight loss (obs. wt. loss, 72.4 ; calc. wt. loss, 73.1%) corresponds to the loss of a ligand molecule and two bromide entities leaving behind mercuric oxide (HgO). The complex **6** shows starts decomposing at slightly lower temperature at 156 ^{o}C and shows complete decomposition of the complex up to 350 ^{o}C .

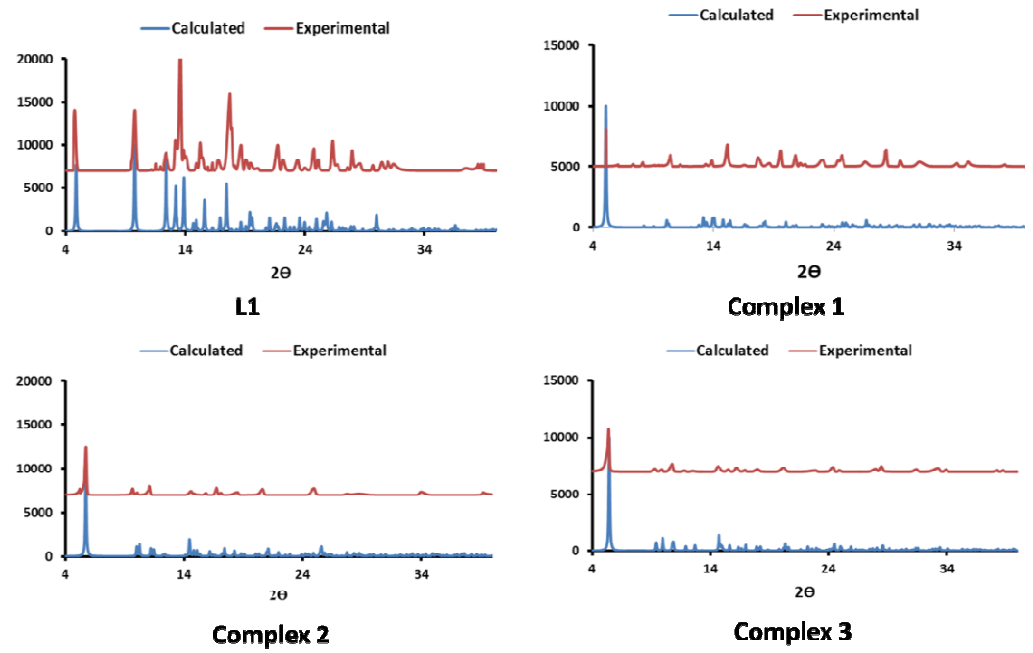

Fig. S18. Calculated & Experimental Powder Diffractograms of **L1** and complexes **1-3.**

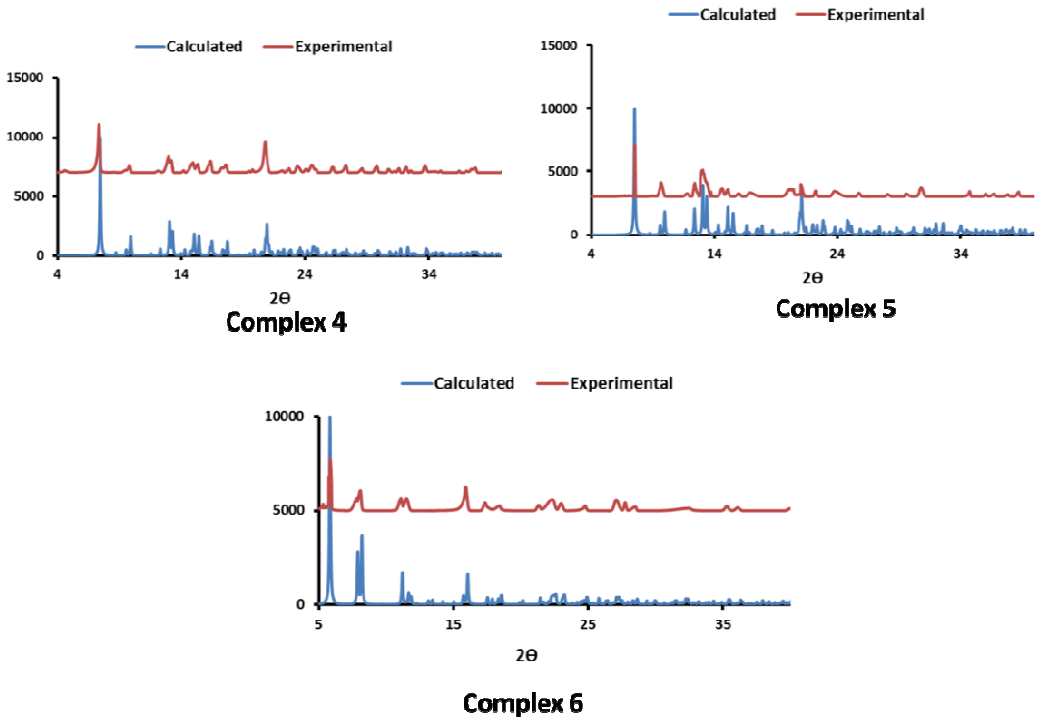

Fig. S19. Calculated & Experimental Powder Diffractograms of complexes **4-6.**